Two Phase Closed Thermosyphon (TPCT) and Its Application for an Air-to-air Heat Exchanger

Wasan Srimuang[1]* Preecha Khantikomol[1] and Pipat Amtachaya[2]

บทคัดย่อ

บทความวิชาการนี้นำเสนอความรู้เกี่ยวกับเทอร์โมไซฟอนที่มีใช้ในปัจจุบันและการประยุกต์ใช้เป็นอุปกรณ์แลกเปลี่ยนความร้อนแบบอากาศกับอากาศ เทอร์โมไซฟอนประกอบด้วยสามส่วน คือ ส่วนทำระเหย ส่วนป้องกันความร้อนและส่วนควบแน่น หลักการทำงานของเทอร์โมไซฟอนเริ่มต้นด้วยสารทำงานที่บรรจุไว้ภายในส่วนทำระเหยได้รับความร้อนจากแหล่งจ่ายพลังงานความร้อนสูง เช่น ความร้อนที่ปล่อยทิ้งจากโรงงานอุตสาหกรรม หรือไอเสียร้อน สารทำงานที่มีสภาวะเป็นของเหลวอิ่มตัวนี้จะเปลี่ยนสถานะเป็นไอลอยขึ้นไปยังส่วนควบแน่น จากนั้นสารทำงานที่มีสถานะเป็นไอที่อยู่ในส่วนควบแน่นจะถ่ายเทความร้อนออกสู่แหล่งรับพลังงานความร้อน เช่น อากาศเย็น หรือน้ำเย็น ทำให้ไอนี้กลั่นตัวกลายเป็นของเหลวและตกลงสู่ส่วนทำระเหย ปัจจุบันมีการประยุกต์ใช้เทอร์โมไซฟอนเป็นอุปกรณ์แลกเปลี่ยนความร้อนแบบอากาศกับอากาศค่อนข้างน้อย เนื่องจากขาดข้อมูลที่เป็นประโยชน์ในการออกแบบและประยุกต์ใช้งาน ดังนั้นบทความนี้จึงนำเสนอรายละเอียดของอุปกรณ์แลกเปลี่ยนความร้อนระหว่างอากาศกับอากาศแบบเทอร์โมไซฟอน สำหรับการนำเอาความร้อนที่เหลือทิ้งจากโรงงานอุตสาหกรรมกลับมาใช้ใหม่ ผลที่ได้จากบทความวิชาการนี้เป็นการเพิ่มข้อมูลสำหรับการออกแบบอุปกรณ์แลกเปลี่ยนความร้อนแบบเทอร์โมไซฟอน

คำสำคัญ: ท่อความร้อน เทอร์โมไซฟอน การนำความร้อนกลับมาใช้ใหม่ เครื่องแลกเปลี่ยนความร้อน

Abstract

This article presents the knowledge of two-phase closed thermosyphon (TPCT) as being used nowadays and the application of TPCT to air to air heat exchanger. The TPCT consists of three parts including the evaporator, adiabatic and condenser sections. The operating process begins at the evaporator section filled with working fluid as a saturated liquid, which is heated by a heat source such as waste heat recovery of industry or exhaust gases. The saturated liquid then changes to vapor and moves up to the condenser section. After that, the

1 Lecturer, Department of Mechanical Engineering, Faculty of Engineering and Architecture, Rajamangala University of Technology Isan.

2 Assistant Professor, Department of Mechanical Engineering, Faculty of Engineering and Architecture, Rajamangala University of Technology Isan.

* Corresponding Author, Tel. 0-4424-2978 Ext.3410, 08-7005-5449, E-mail: wasansrimuang@hotmail.com

Received 29 April 2011; Accepted 2 August 2011

vapor in the condenser section transfers the heat to a heat sink such as cold air or cold water. As a result, the vapor condenses to a liquid and flows down to the evaporator section. Currently, the TPCTs show a few applications for an air to air heat exchanger due to inadequate information for the design and application. Therefore, the purpose of this article is to present information of the particular TPCTs, which is an air to air heat exchanger for heat recovery form waste heat of industry. The result of this article could be advantageous for further design of TPCT heat exchanger.

Keyword: Heat Pipe, Thermosyphon, Heat Recovery, Heat Exchanger

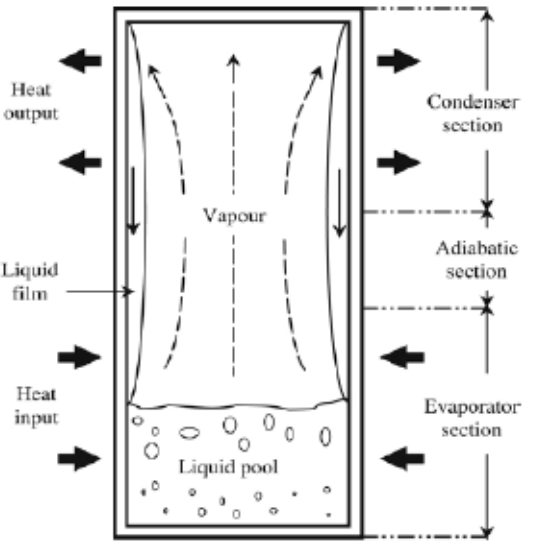

Figure1 Schematic diagram of working fluid in the CTPCT [1].

1. Introduction

The two-phase closed thermosyphon (TPCT), also referred to as conventional two phase closed thermosyphon (CTPCT) or wickless heat pipe (HP) is a type of heat exchanger. It can transfer heat by itself with the latent heat of working fluid in the tubes. The CTPCT consists of three parts, i.e. the evaporator, adiabatic, and condenser sections.

When the working fluid as liquid phase at the evaporator section is heated by a heat source such as waste heat, the liquid changes to vapor and moves up to the condenser section. Then, the vapor in the condenser section transfers the heat to a heat sink such as cooled air. A schematic of the working principle of the CTPCT is shown in Fig. 1.

The CTPCT heat exchangers bear significant advantages over general heat exchangers since they do not require any external energy. Moreover, they have a high rate of effectiveness with less maintenance problems owing to containing non-moving parts. With appropriate working fluid, they are able to operate even when the temperature difference between the heat source and the heat sink is very small. The CTPCT is the best choice with virtually cross leakage between the exhaust gases and supply air. Heat exchangers with CTPCT units have advantages in terms of relative economy, less drop pressure of fluid flow, complete separation of hot and cold fluids, and high reliability. The CTPCT have been extensively applied in many industries such as energy engineering, chemical engineering and metallurgical engineering as waste heat recovery systems. Fig.2 shows an application of CTPCT as air to air heat exchanger is the recovery of the heat from exhaust gases of furnace.

Fig. 2a shows the exhaust gases out off the stack of furnace, which flow into the surrounding. They are waste energy and cause damages to the environment. The CTPCT heat exchanger is applied for heat recovery. It is an air pre-heater, which couples on the stack of the

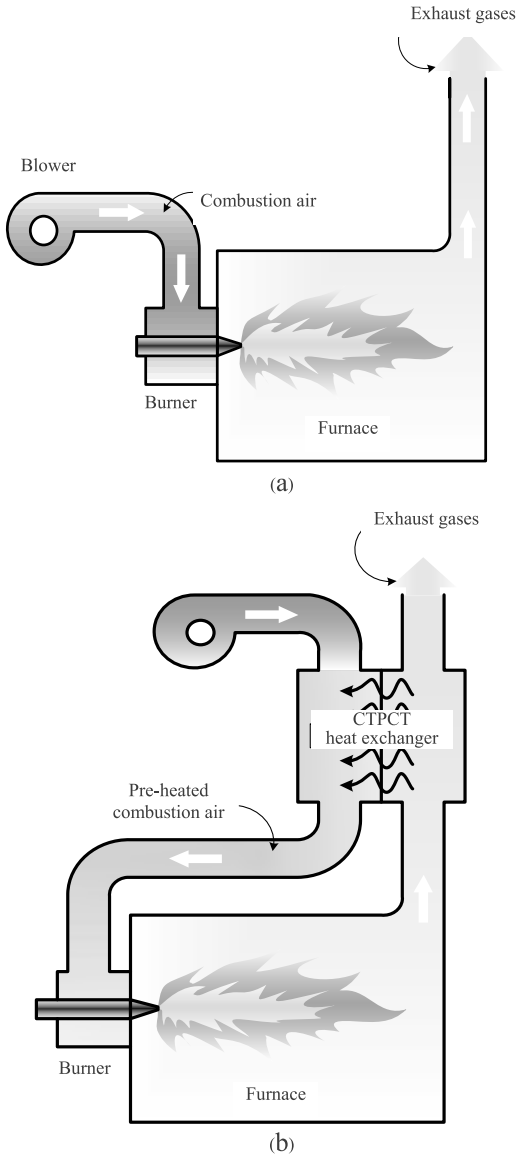

Figure 2 Waste heat recovery from exhaust gases.

furnace and fresh air supply into burner. This device transfers the heat from exhaust gases to the incoming air for combustion. Moreover, the waste heat recovery by using CTPCT is an excellent way for reducing energy consumption.

The problems of engineers involve application the CTPCT as heat exchanger for heat recovery: how to design and calculate the heat transfer rate of CTPCT heat exchanger, how to calculate the pressure drop on air side of CTPCT heat exchanger, and how to evaluate the effectiveness of the mentioned device. This review article presents the knowledge of thermosyphons technology. The various researches on CTPCTs and flat two-phase closed thermosyphons (FTPCTs) are summarized and the calculation involving heat transfer rate of CTPCT and FTPCT will be explained.

In addition, several researches on the applications of CTPCT air to air heat exchangers for heat recovery are presented and discussed in more details.

Finally, the parametric on the effectiveness and pressure drop characteristics of CTPCT air to air heat exchangers will be described.

Many basic researches related to the CTPCTs [2]-[13] and FTPCTs [14],[15] have been published. Based on their studies, the geometric characteristics with working fluids of CTPCTs and FTPCTs for these researches are compared in Table 1, whereby the data become beneficial for the designers and researchers.

2. Heat Transfer Rate of CTPCT and FTPCT

The calculation of the heat transfer rate for CTPCT is presented by Parametthanuwat et al. [16]. An equation based on non-dimensional parameters for prediction the thermal performance of CTPCTs can be illustrated as the following:

$$q = 3.11\left[\frac{L_e}{d_i}\frac{Pr^{2.2}\,Bo^{2.5}Ja^{2.1}We^{1.4}Fr^{1.4}Co^{2.5}Nu^{2.5}}{Ar^{0.5}Gr^{0.5}}\right]^{0.13} \times\left[\rho_v h_{fg}\left(\frac{\rho_l-\rho_v}{\rho_v^2}\right)\right]^{\frac{1}{4}} \quad (1)$$

The equation (1) with the standard deviation of 5% is suggested by the researchers [16]

Table 1 The significant detail of the CTPCTs and FTPCTs

	Pipe	**Working fluid/FR**	**Authors**
CTPCT	Material : copper, outside diameter : 28 mm, inside diameter : 25 mm L_e : 300 mm, L_a : 180 mm L_c : 300 mm	Material : R-22, R-134a, water FR : 50-80% of the evaporator section	Ong and Alalhi [2]
CTPCT	Material : copper, inside diameter : 7.5, 11.1, and 25.4 mm. $L_e = L_a = L_c$, L_e/d_i = 5, 10, 20, 30 and 40	Material : water, R-22, R-123, R134a, and ethanol FR : 50, 80 and 100% of the evaporatorsection	Payakaruk et al. [3]
CTPCT	Material : copper, outside diameter : 25 mm, inside diameter : 23 mm L_t : 900 mm L_a : 275, 325, 350 mm L_c : 300 mm	Material : water, R-134a FR : 40-80% of the evaporator section	Ziyan et al. [4]
CTPCT	Material : copper, outside diameter : 22.23 mm, ceramic, outside diameter : 32.7 mm, L_e : 105 mm, L_a : 75 mm L_c : 420 mm	Material : C_6F_{14} FR : 10-70% of the evaporator section	Park et al. [5]
CTPCT	Material : aluminum for L_e, outside diameter : 50 mm, wall thickness : 20 mm L_e : 300 mm. Pyrex tube for L_a and L_c, inside diameter : 50 mm, wall thickness : 4 mm, L_a : 150 mm, L_c : 500 mm	Material : n-pentane FR : 33, 66, 100% of the evaporator section	Farsi et al. [6]
CTPCT	Material : copper, out side diameter : 15 mm inside diameter : 12 mm L_e : 25 mm, L_c : 41 mm	Material : water, R-134a. FR :50% of the evaporator section	Wangnipparnto et al. [7]
CTPCT (Case 1)	Material : stainless steel, outside diameter : 0.8 mm, inside diameter : 0.6 mm L_e : 10 mm, L_a : 9 mm L_c : 3 mm	Material : nitrogen, FR : 4.5-20.2% of the total volume	Jiao et al. [8]
CTPCT (Case 2)	Material : stainless steel, outside diameter : 1 mm, inside diameter : 0.8 mm L_e : 5 mm, L_a : 45 mm L_c : 10 mm	Material : nitrogen, FR : 4.5-20.2% of the total volume	

Table 1 The significant detail of the CTPCTs and FTPCTs (continue)

	Pipe	**Working fluid/FR**	**Authors**
CTPCT	Material : copper, outside diameter : 19.0 mm inside diameter: 17.5 mm L_e : 400 mm, L_a : 200 mm, L_c : 400 mm	Material : Water vapor, air FR : 30-80% of the total volume	Alizadeh dakhel et al. [9]
CTPCT (Case A)	Outside diameter : 28.6 mm, inside diameter : 26.0 mm Material : L_e : 250 mm (copper) L_a : 280 mm (copper) L_c : : 240 mm (copper)	Material : R-134a, FR : 25-85% of evaporator section	Guo and Nutter [10]
CTPCT (Case B)	outside diameter : 28.6 mm, inside diameter : 26.0 mm Material : L_e : 250 mm (copper) L_a : 280 mm (polycarbonate) L_c : : 240 mm (copper)	Material : R-134a, FR : 25-85% of evaporator section	
CTPCT	Material : stainless, inside diameter : 25.4 mm L_e : 30 cm L_c : : 120 cm	Material : silver nano-water mixture. FR : 80% of the evaporator section	Parametthanuwat et al. [11]
CTPCT	Material : copper, outside diameter : 22 mm inside diameter: 20 mm L_e : 400 mm, L_a : 200 mm, L_c : : 400 mm	Material : Water FR : 75% of the total volume	Rahimi et al. [12]
CTPCT	Material : copper, outside diameter : 15 mm inside diameter: 20 mm L_e : 100 mm, L_a : 100 mm, L_c : 150 mm	Material : CuO- nano with water, FR : 50% of evaporator section	Liu et al. [13]
FTPCT	Material : copper, inside diameter: 32 mm, wall thickness : 3.2 mm L_e : 300 mm, L_a : 100 mm, L_c : 380 mm	Material : water FR : 30-90% of evaporator section	Amtachaya and Srimuang [14]
FTPCT	Material : copper, inside diameter: 8.6 mm, wall thickness : 0.46 mm $L_e = L_a = L_c$ L_e : 130, 230 and 330 mm	Material : water, ethanol, and R-123 FR : 20-80% of total volume	Ritidech and Srimuang [15]

For the FTPCT, Rittidech and Srimuang [15] reported the correlation based on non-dimensional parameters for predicting the heat transfer rate of FTPCT. The heat rate has been calculated as follows:

$$q = 0.0144\left[\left(\frac{L_e}{4R}\right)^{0.9} P_4^{\frac{1}{4}}{}^{\frac{2}{f}} Bo^4 Ja^{1.8}\left(\frac{\rho_v}{\rho_l}\right)^{1.8}\right]^{0.13} \times\left[\rho_v h_{fg}\left(\frac{\rho_l - h\,\rho_v}{\rho_v^2}\right)\right] \quad (2)$$

The equation (2) within ± 25% standard deviation is recommended by the researchers [15].

3. Literature Applications of CTPCT for Heat Recovery

Since the late 1990s, a number of research works have applied the CTPCT for heat recovery, in which the improved effectiveness of CTPCT air to air heat exchanger have been proposed. Several investigations are of our much interest. Lukitobudi et al. [17] presented the design, construction and testing of a CTPCT air to air heat exchanger for medium temperature heat recovery in a bakery as shown in Fig.3. The maximum effectiveness of this CTPCT is 0.80.

Yang et al. [18] used the CTPCT heat exchanger for a comfortable temperature in a carriage by using exhaust gas as heat source. The CTPCT heat exchanger of [18] is shown in Fig. 4. The experimental and results were exposed in compliance.

Noie and Majideian [19] reported the waste heat recovery using the CTPCT heat exchanger for surgery rooms in hospitals. The CTPCT heat exchanger is shown in Fig. 5. It was designed for a low temperature ambiance (15-55°C). The result pointed out a minor CTPCT effectiveness of 0.16, due to the fact that it was tested under low temperature of the heat source.

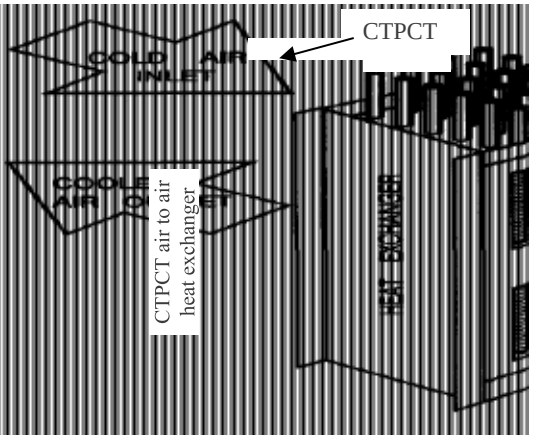

Figure 3 The CTPCT air-to-air heat exchanger, as stated by Lukitobudi et al. [17].

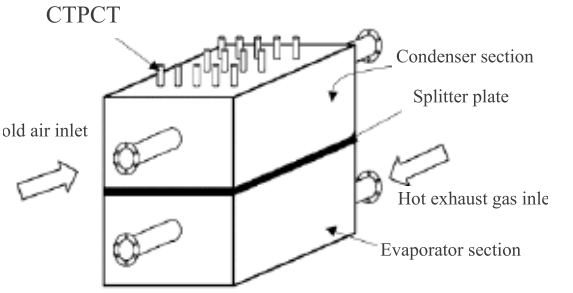

Figure 4 The CTPCT heat exchanger in accordance with Yang et al. [18].

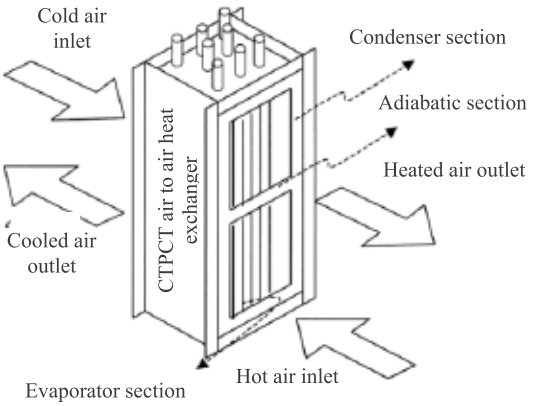

Figure 5 The CTPCT heat exchanger in line with Noie and Majideian [19].

Figure 6 The CTPCT for an air to air heat exchanger, as indicated by Noie [20].

Noie [20] also reported the effectiveness of CTPCT air to air heat exchanger. His CTPCT heat exchanger is shown in Fig. 6.

As mentioned above [17-20], the CTPCTs applied in the four studies were illustrated with a similar diameter of 15 mm. On the other hand, the CTPCT heat exchanger length of each study was varied. Yang at el. [18] employed 310 mm. tubes whereas Lukitobudi et al. [17], and Noie and Majideian [19] utilized those of 650 and 600 mm. long. With regard to Noie [20], the longer tubes of 1300 mm. were put into operation. A number of materials and details including working fluid types, filling ratio, material tube, fin types, together with mesh and evaporator length of preceding studies are summarized in Table 2.

4. Heat Transfer Rate on Air Side of CTPCT Air to Air Heat Exchanger

In the CTPCT air to air heat exchanger, working fluid moves up and down inside the CTPCT while the hot and cooled air move over the tubes in a perpendicular direction. The tubes in the tube bank are usually placed in an evaporator and condenser boxes. In this section, general aspects of flow over a tube bank are demonstrated in effort to generate insightful understanding on CTPCT heat exchanger functioning as far as the tubes are concerned. Flow through the tubes can be calculated by multiplying the amount of air flow through a single tube by the number of tubes. This is not the case for flow over the tubes, however. As a matter of fact, the tubes affect the flow pattern and turbulence level downstream, and thus the transfer of heat occurs either to or from them. Therefore, when analyzing heat transfer to or from a tube bank in cross flow, all the tubes in the bundle will be taken into account. The tubes in a tube bank are usually arranged either in-line or staggered in the direction of flow, as shown in Fig.7.

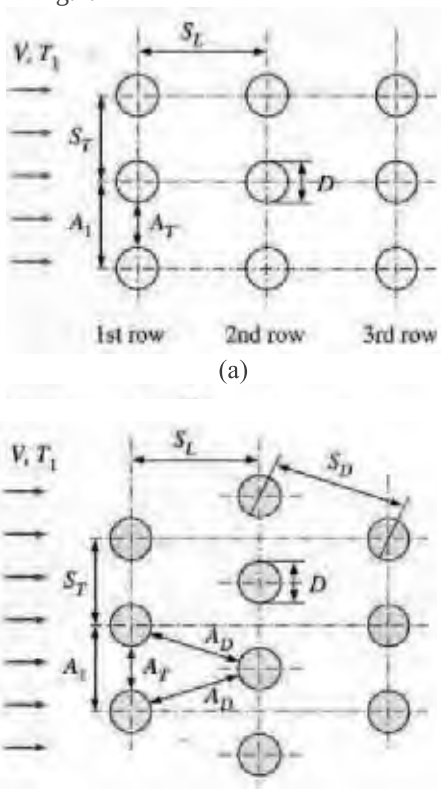

Figure 7 Arrangements of the tubes in in-line and staggered tube banks (a) in-line (b) staggered [21]

Table 2 The summation of available CTPCT air to air heat exchangers

	Pipe	Working fluid/FR	Fins	Wick	Authors
Case 1	Material : copper Out side diameter : 15.88 mm Wall thickness : 1.22 mm L_e : 300 mm L_a : 300 mm L_c : 300 mm	Material : water FR : 60% of the evaporator section	Type : continuous fin Material : - copper : evaporator section - aluminum : condenser section Spacing : 472 fins per meter Thickness : 0.162 mm	none	Lukitobudi et al. [17]
Case 2	Material : steel Out side diameter : 26.27 mm Wall thickness : 7.65 mm L_e : 300 mm L_a : 150 mm L_c : 300 mm	Material : water FR : 60% of the evaporator section	Type : circular spiral fin Material : steel Spacing : 315 fins per meter Thickness : 0.8 mm Diameter : 52.7 mm	none	
Case 3	Material : copper Out side diameter : 15.88 mm Wall thickness : 1.22 mm L_e : 300 mm L_a : 150 mm L_c : 300 mm	Material : water FR : 60% of the evaporator section	none	none	
	Material : steel Out side diameter : 20 mm Wall thickness : 1.5 mm L_e : 150 mm L_a : 5 mm L_c : 150 mm Length for the end condenser section : 5 mm	Material : water FR :35% of the evaporator section	Type : plate fin Material : steel Spacing : 315 fins per meter Thickness : 1.5 mm Height : 8 mm	none	Yang et al. [18]
	Material : copper Out side diameter : 15 mm Wall thickness :3 mm L_e : 300 mm L_t : 600 mm L_c : 300 mm	Material : methanol Maximum working pressure: 2.3 bar.	none	100 mesh SS, 50 mesh nickel, 250 mesh nickel	Noie and Majideian [19]
	Material : copper Out side diameter : 15 mm inside diameter : 14 mm L_e : 600 mm L_a : 100 mm L_c : 600 mm	Material : water FR :90% of the evaporator section	Type : plate fin Material : aluminum Spacing : 300 fins per meter Thickness : 0.4 mm	none	Noie [20]

The outer tube diameter (D) is taken as the characteristic length. The arrangement of the tubes in the tube bank is characterized by the transverse pitch (S_T), longitudinal pitch (S_L), and the diagonal pitch (S_D) between tube centers. The diagonal pitch is determined from:

$$S_D = \sqrt{S_L^2 + (S_T/2)^2} \ . \qquad (3)$$

As the fluid enters the tube bank, the flow area decreases from $A_l = S_T L$ to $A_T = (S_T - D)L$ between the tubes leading to an increase in flow velocity. In a staggered arrangement, the velocity may increase further in the diagonal region if the tube rows are very close to each other. In tube banks, the flow characteristics are dominated by the maximum velocity V_{max} that occurs within the tube bank rather than the approach velocity (V). Therefore, the Reynolds number is defined on the basis of maximum velocity as:

$$R_{ed} = \frac{\rho V_{max} D}{\mu} = \frac{V_{max} D}{\nu} \ . \qquad (4)$$

The maximum velocity is determined from the conservation of mass requirement for steady incompressible flow. For an in-linearrangement, the maximum velocity occurs at the minimum flow area between the tubes, and the conservation of mass can be expressed as $\rho V A_l = \rho V_{max} A_T$ or $V S_T = V_{max}(S_T - D)$. T Then the maximum velocity becomes:

$$V_{max} = \frac{S_T (V)}{S_T - D} \ . \qquad (5)$$

In the staggered arrangement, the fluid approaching through area (A_l) in Fig.7b passes through area (A_T) and then through area $2A_D$ as it warps around the pipe in the next row. In case of $2A_D > A_T$, the maximum velocity will still occur at A_T between the tubes, and thus the V_{max} of equation (6) can also be used for staggered tube banks. In case of $2A_D > A_T$, (or, if $2(S_D - D) < (S_T - D)$), the maximum velocity will occur at the diagonal cross section, and the maximum velocity in this case becomes:

$$V_{max} = \frac{S_T (V)}{2(S_T - D)} \ . \qquad (6)$$

Therefore, each tube in a tube bank that consists of a single transverse row can be treated as a single tube in cross-flow. The nature of flow around a tube in the second and subsequent rows is greatly different, however, because of wakes formed and the heat transfer coefficient, increases with row number due to the combined effects of upstream rows. But there is no significant change in turbulence level after the first few rows, and thus the heat transfer coefficient remains constant. Flow through tube banks is studied experimentally since it is too complex to be treated analytically. The average heat transfer coefficient for the entire tube bank, which depends on the number of tube rows along the flow as well as the arrangement and the size of the tubes are of interest. Several correlations, all based on experimental data, have been proposed for the average Nusselt number for cross flow over tube banks. More recently, Zukauskas [22] has proposed a correlation whose general form is:

$$Nu_d = \frac{hD}{k} = C\, Re_D^m Pr^n (Pr/Pr_s)^{0.25} \ . \qquad (7)$$

where the values of the constants C, m and n depend on Reynolds number. Correlation patterns are given in Table 3 for $0.7 < Pr < 500$ and $0 < R_e D < 2\ 10^6$.

Table 3 Nusselt number correlations for cross flow over tube banks for N >16 and 0.7 < Pr < 500 [22].

Arrangement	Range of R_{ed}	Correlation of N_{uD}
In-line	0-100	$0.9R_{eD}^{0.4}\,Pr^{0.36}(Pr/Pr_s)^{0.25}$
	100-1000	$0.52R_{eD}^{0.5}\,Pr^{0.36}(Pr/Pr_s)^{0.25}$
	1000-2×10^5	$0.9R_{eD}^{0.4}\,Pr^{0.36}(Pr/Pr_s)^{0.25}$
	2×10^5-2×10^6	$0.033R_{eD}^{0.8}\,Pr^{0.4}(Pr/Pr_s)^{0.25}$
Staggered	0-500	$1.04R_{eD}^{0.4}\,Pr^{0.36}(Pr/Pr_s)^{0.25}$
	500-1000	$0.71R_{eD}^{0.5}\,Pr^{0.36}(Pr/Pr_s)^{0.25}$
	1000-2×10^5	$0.35(S_T/S_L)^{0.2}$ $\times R_{eD}^{0.6}\,Pr^{0.36}(Pr/Pr_s)^{0.25}$
	2×10^5-2×10^6	$0.31(S_T/S_L)^{0.2}$ $\times R_{eD}^{0.8}\,Pr^{0.36}(Pr/Pr_s)^{0.25}$

The uncertainty in the values of Nusselt number obtained from these relations is ± 15 percent. Note that all properties except Pr_s are to be evaluated at the arithmetic mean temperature of the fluid determined from $T_m = (T_{in} + T_{out})/2$ where T_{in} and T_{out} are the fluid temperatures at the inlet and the exit of the tube bank, respectively. Once the Nusselt number and thus the average heat transfer coefficient for the entire tube bank are known, the heat transfer rate can be determined from Newton's law of cooling using a suitable temperature difference; $\Delta T = T_s - T_{avg} = T_s = (T_{in} + T_{out})/2$. This will, in general, over predict the heat transfer rate. The proper temperature difference for internal flow (flow over tube banks is still internal flow through the shell) is the logarithmic mean temperature difference ΔT_{ln} defined as :

$$\Delta T_{ln} = \frac{(T_s - T_{out}) - (T_s - T_{in})}{\ln[(T_s - T_{out})/(T_s - T_{in})]} = \frac{\Delta T_{out} - \Delta T_{in}}{\ln(\Delta T_{out}/\Delta T_{in})}. \quad (8)$$

The exit temperature of the fluid Te can also be determined by the following equation:

$$T_{out} = T_s - (T_s - T_{in})\exp(\pm\frac{A_s h}{\dot{m}C_P}), \quad (9)$$

where $A_s = N\pi DL$ is the heat transfer surface area and in $\dot{m} = \rho V(N_T S_T L)$ is the mass flow rate of the fluid. Here, N is the total number of tubes in the bank, N_T is the number of tubes in a transverse plane, L is the length of the tubes, and V is the velocity of the fluid just before entering the tube bank. Then the heat transfer rate can be determined from :

$$\dot{Q} = hA_s\Delta T_{ln} = \dot{m}C_P(T_{out} - T_{in}). \quad (10)$$

The second relation is usually more convenient to use since it does not require the calculation of ΔT_{ln}.

5. Effectiveness of CTPCT Air to Air Heat Exchanger

Thermal performance is the governing factor in choosing the CTPCT air to air heat exchangers for heat recovery. When the CTPCT was used to air-to-air heat exchanger, it must also meet the operation requirement under various conditions. The effectiveness is based on the principle that the actual heat transfer occurring between the fluids is the fraction of the maximum heat transfer possible. The maximum heat transfer possible could be theoretically achieved with a counter flow heat exchanger of infinite surface area. Heat exchanger effectiveness (ε) is defined as:

$$\varepsilon = \frac{\dot{Q}_{actual}}{\dot{Q}_{max}} = \frac{\text{Actual heat transfer rate}}{\text{Maximum possible heat transfer rate}}. \quad (11)$$

The actual heat transfer rate in a heat exchanger can be determined from an energy balance on the hot or cold fluids and can be express as:

$$\dot{Q}_{actual} = \dot{m}_c C_{p,c}(T_{c,out} - T_{c,in}) = \dot{m}_h C_{p,h}(T_{h,in} - T_{h,out}), \quad (12)$$

where $\dot{Q}_{actual}$ is actual heat transfer rate, $\dot{Q}_{max}$ is maximum possible heat tranfer rate of heat exchanger $\dot{m}$, C_p a.,, and T are mass flow rate, specific heat and temperature of fluid flow through a heat exchanger, respectively. The effectiveness line the length $0 \le \varepsilon \le 1$.

If $C_c < C_h$, $C_c = (\dot{m}C_p)_c$, and $C_h = (\dot{m}C_p)_h$.

$$\varepsilon = \frac{(T_{c,out} - T_{c,in})}{(T_{h,in} - T_{c,in})}. \quad (13)$$

If $C_h < C_c$,

$$\varepsilon = \frac{(T_{h,in} - T_{h,out})}{(T_{h,in} - T_{c,in})}, \quad (14)$$

In previous works, the effectiveness of CTPCT heat exchange is calculated by employing equation (13) or (14). The CTPCT heat exchanger's effectiveness of those four researchers is shown in Table 4. These are useful data for the designers to select some optimal conditions to apply the CTPCT heat exchanger for heat recovery system.

6. Pressure Drop on Air Side of CTPCT Air to Air Heat Exchanger

The pressure drop (ΔP) on air side of CTPCT air to air heat exchanger is the difference between the pressure at the inlet and the exit of the tube bank. It is a measurement of the resistance the tubes offer flow over them, and is expressed as:

$$\Delta P = N_L f \chi \frac{\rho V_{max}^2}{2}, \quad (15)$$

where f and χ are the friction and correction factors respectively. Fig. 8 shows the relation of f and χ against the Reynolds number based on the maximum velocity V_{max}.

The friction factor in Fig. 8a is for a square inline tube bank ($ST = S_L$), and the correction factor given in the insert is used to account for the effects of the deviation of rectangular inline arrangements from square arrangement. Similarly, the friction Factor in Fig.8b is for an equilateral staggered tube bank ($S_T = S_D$), and the correction factor is to account for the effects of deviation from equilateral arrangement. At $\chi = 1$, obviously, both are square. Pressure drop also occurs in the flow direction, and thus N_L (The number of rows) was used in the ΔP relation. The power required to move the fluid through a tube bank is proportional to the pressure drop. When the pressure drop is available, the pumping power required can be determined from:

$$\dot{W}_{pump} = \dot{V}\Delta P = \frac{\dot{m}\Delta P}{\rho}. \quad (16)$$

where $\dot{V} = V(N_T S_T L)$ is the volume flow rate and $\dot{m} = \rho\dot{V} = \rho V(N_T S_T L)$ is the mass flow rate of the fluid flowing through the tube bank. Note that the power required to keep a fluid flowing through the tube bank (and thus the operating cost) is proportional to the pressure drop. Therefore, the benefits of enhancing heat transfer in a tube bank via rearrangement should be weighed against the cost of additional power requirements. However, only tube banks (no fins) is considered. Tube banks with finned surfaces are also commonly used in practice, especially when the fluid is gas, and heat transfer and pressure drop correlations can be found in the literature for tube banks with plate fins, wavy plate fins, strip fins, etc.

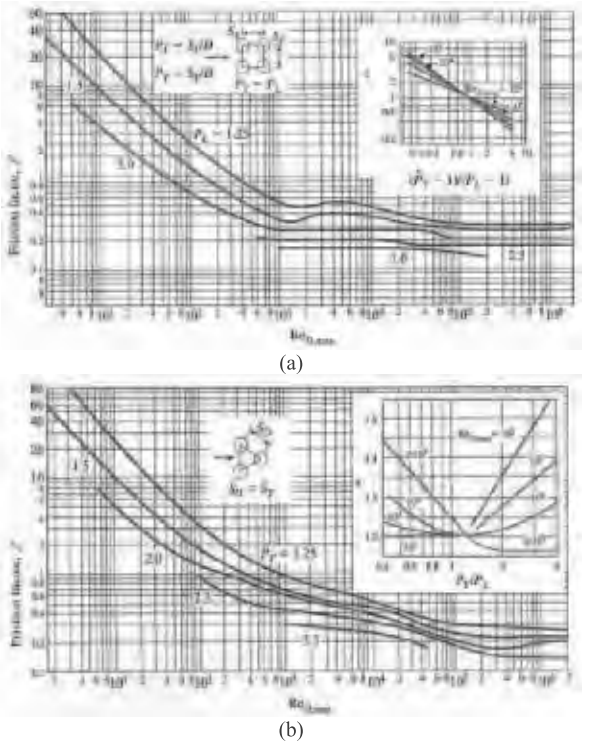

Figure 8 Friction factor *f* and correlation factor χ for tube banks (a) in-line (b) staggered [22].

Research articles about the pressure drop on air side of CTPCT air to air heat exchanger seem very scarce. If the pressure drops on air side of CTPCT heat exchanger and the fin-tube heat exchanger (FTHE) is taken into account, there is no difference between CTPCT and FTHE. Therefore, the information of FTHE can be used for the CTPCT heat exchanger. Studies on the pressure drop on the air side of the FTHE have been reported in Mendez et al. [23], Wang and Chi [24] and Tao et al. [25],[26]. Mendez et al. [23] investigated the effect of the fin spacing on the total heat transfer rate and pressure drop for a single row of the FTHE by using flow visualization and numerical computation techniques. The results showed that for small fin spacing, the nature of the flow remarkably changes as the fin spacing increases. Wang and Chi [24] experimentally determined the effects of circular tube rows, fin pitch, and tube diameter on heat transfer and pressure drop of the FTHE. They found that the heat transfer performance is improved with the decrease of fin pitch. The effect of tube row on the heat transfer performance is especially pronounced at low Reynolds number where the number of tube rows is large and the fin pitch is small. Tao et al. [25],[26] numerically studied the effects of Reynolds number, fin pitch, wavy angle, and tube row number on heat transfer coefficient and efficiency of the FTHE. They found that, as the wavy angles increase and the fin pitch and tube row number decrease, the heat transfer of the finned tube bank are enhanced with some penalty in pressure drop.

Based on their studies [23]-[26], it can be concluded that the geometries of fin-tube, fin pitch, value of Reynolds number of the frontal air, and tube row number yield significant effects on the pressure drop characteristics of the FTHE. Therefore, these parameters should be considered while designing.

7. The Parametric on the Effectiveness of CTPCT Air to Air Heat Exchanger

The taste rigs for the tests of the performance of CTPCT and the parametric on the effectiveness of CTPCT air to air heat exchanger of various researches involved in the area of CTPCT heat exchanger are highlighted in this section. A test rig of Lukitobudi et al. [17] is an interesting research work of which the study on the effectiveness of the CTPCT heat exchanger is shown in Fig.9. In this figure, the cold fluid flows into the condenser section, while the hot fluid flows through the evaporator one. Some other

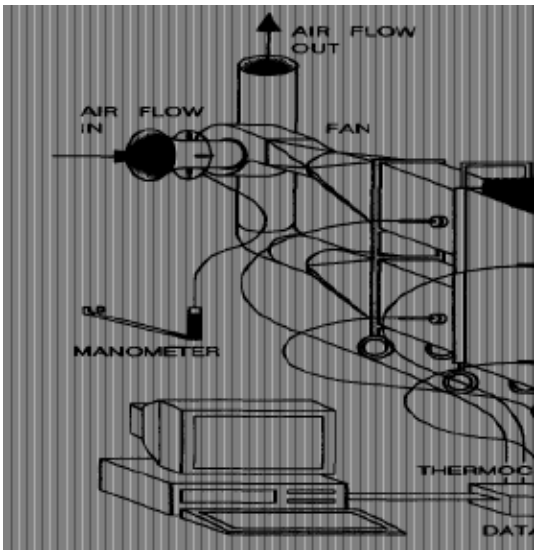

Figure 9 The test rig of the CTPCT air to air heat exchanger [17].

experimental apparatuses of [18],[19] are similar to [17]. In the experimental setup of Noie and Majideian [19], after both fluids flow through CTPCT, it directly flow into environment. For the experimental setup of Yang et al. [18], after the exhaust gases flow through the evaporator section, they flow directly to environment, while the cold air circulate which contrasts to the experiment of Noie [20].

For the application of CTPCT heat exchanger in heat recovery, the waste heat energy such as exhaust gases flowing through the evaporator section should subsequently flow right away to environment, the same as the experimental setup of Yang et al. [18] or similar to Fig. 2b.

Based on their studies [17]-[19], many parameters such as filling ratio, types of working fluid, inlet air velocity and temperature into evaporator section, material types and dimensions of fin and tube, various lengths of the evaporator section, condenser section and adiabatic section affect the effectiveness of the CTPCT air to air heat exchanger. Studies on the parameters are considered as controlled parameters or variable parameters. From the previous researches [17]-[20] on using the CTPCT and HP as the heat recovery, the parameters and effectiveness are also compared in Table 4. It can be concluded that the effectiveness of the CTPCT air to air heat exchanger depends on four main factors as follow:

Table 4 Comparison of control/variable parameters and the effectiveness for the various CTPCT air to air heat exchangers

Type	Control parameters	Variable parameters	Authors	Effectiveness
TPCT	- cold air, T = 20 ^{o}C - filling ratio = 60% - working fluid is water	- hot and cold air, V = 1.5-5.5 m/s - material of tubes - material and type of fins - heat input of, $\dot{Q}$ = 4-20 kW	Lukitobudi et al. [17]	0.18-0.80
TPCT	- cold air velocity - filling ratio = 35%	- exhaust gas temperature of 100 – 300^{o}C	Yang et al. [18]	0.28
HP	- cold air, V = 2.3 m/s - hot air, V = 2.3 m/s - filling ratio	- working fluid - type of wicks	Noie and Majideian [19]	0.16
TPCT	- cold air T 25 ^{o}C - filling ratio = 60% - working fluid is water - cold air, V 2.3 m/s	- hot air, $100 \leq T \leq 250$ ^{o}C - hot air, $0.5 \leq V \leq 5.5$ m/s - heat input, $18 \leq \dot{Q} \leq 72$ kW	Noie [20]	0.37-0.65

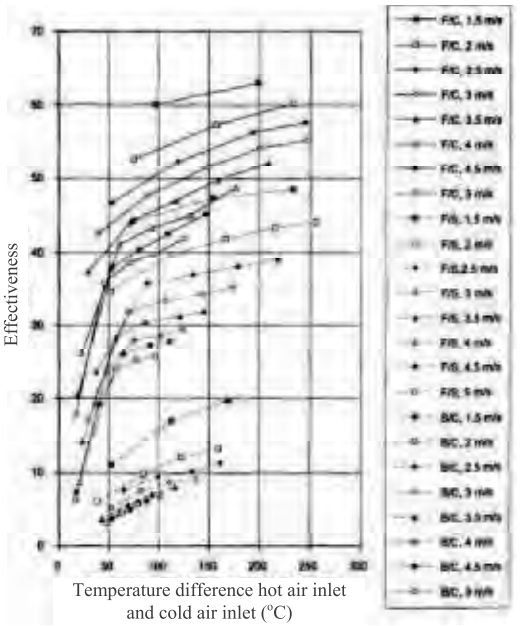

Figure 10 Effect of inlet temperatures in evaporator on effectiveness [17].

1. The inlet temperatures in the evaporator have an effect to the effectiveness. This effect can be confirmed by a reported of Lukitobudi et al. [17]. They presented that the effectiveness increases with increasing temperature across air to air heat exchanger. Their result is shown in Fig. 10, which is similar to those of previous study of [20].

2. The hot and cold air velocities flow through the evaporator and condenser section respectively. In accordance with Noie [20]: the minimum effectiveness is put forward as $C_h = C_c$ whereby the heat rate capacity is not different. Therefore, for the better performance of heat exchanger at the equal condenser and evaporator sections, air face velocities should be avoided. This result is exposed in Fig. 11. Moreover, the effectiveness increases with decreasing hot air velocity. These results are in conformity with earlier studies [28], notwithstanding some difference in tube length and

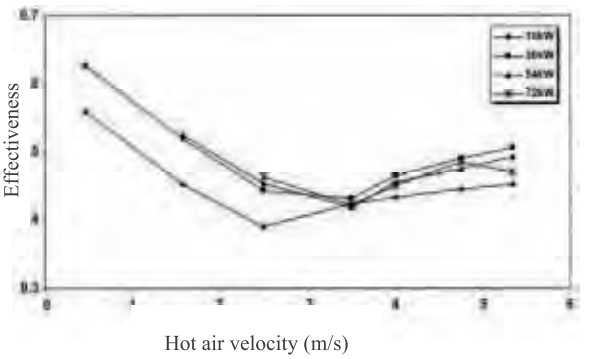

Figure 11 Effect of hot air velocities flow into the evaporator on effectiveness [20].

experimental conditions.

3. The geometrical fin, an arrangement of the tubes such as an in-line and staggered tube banks, and fin or tube space have a considerable impact on the effectiveness of the CTPCT air to air heat exchanger [27],[28].

4. Thermal performance of CTPCT is a significant factor on the effectiveness of the CTPCT heat exchanger. The CTPCT's effectiveness increases in conjunction with the thermal performance or efficiency of CTPCT.

8. Conclusion

This review article presents the application the CTPCT for heat recovery, it can be concluded that;

- The CTPCT air to air heat exchanger can be applied to heat recovery. The CTPCT heat exchangers appear to outperform general heat exchangers given that they do not require any external energy. Additionally, owing to their non-moving parts, the devices are regarded more effective with less maintenance problems
- The temperature of heat source contributes to the efficiency of CTPCT air to air heat exchanger. The effectiveness increases along with the temperature of the heat source.
- The hot and fresh air velocities play a significant

role on CTPCT air to air heat exchanger efficacy. The minimum effectiveness occurs with the equal air flow between hot air stream and fresh air velocity.

● The effectiveness of CTPCT air to air heat exchanger was displayed in the range 0.16-0.80, depending on the design, conditioning operation and the thermal performance of CTPCT.

● The pressure drop characteristic of CTPCT air to air heat exchanger depends on the inlet air velocities that flow through the CTPCT heat exchanger, geometrical fin, and arrangement of tubes in a tube bank. In addition, the pressure drop increases with frontal air velocity, and decreases with increasing fin space.

● This article raises awareness of the selection of CTPCT air to air heat exchanger with the optimum parameters, which, in turn instigate promising advantages in terms of ultimate energy efficiency as well as overall cost effectiveness.

9. Nomenclature

A_s heat transfer surface area (m^2)

Ar Archimedes number, $\left(\frac{g\rho_s L^3}{\mu^2}(\rho_s-\rho_f\right)$

Bo Bond number, $\left(d_i\left[g\left(\frac{\rho_l-\rho_v}{\sigma}\right)\right]^{\frac{1}{2}}\right)$

C heat rate capacity (kJ/s K) or constant value

C_p constant pressure specific heat (kJ/kg ^oC)

Co Condensation number, $\frac{h}{k}\left[\frac{\mu^2}{g\rho^2}\right]^{\frac{1}{3}}$

d, D diameter (m)

f friction factor

Fr Froude number,

FR filling ratio (%) $\left(\frac{Q^2}{\rho_v^2(d_i)^5 h_{fg}{}^2 g}\right)$

g gravitational acceleration (m/s^2)

Gr Grashof number, $\frac{L^3\rho^2\beta\Delta TC_p}{\mu^2}$

h heat transfer coefficient ($kW/m^{2o}C$)

h_{fg} latent heat of vaporization (kJ/kg)

Ja Jacob number, $\left(\frac{h_{fg}}{C_{p\,l}T}\right)$

k thermal conductivity (kW/m K)

L length of tube (m)

$\dot{m}$ mass flow rate, kg/s

N number of rows

Nu Nusselt number, $\frac{hd}{k}$

P pressure (Pa)

Pr Prandtl number, $\left(\frac{\mu_l C_{p,l}}{k_l}\right)$

$\dot{Q}$ heat transfer rate (W)

q heat flux (kW/m^2)

R_h hydraulics radius (m)

S_D diagonal pitch (m)

S_L longitudinal pitch (m)

S_T transverse pitch (m)

T temperature (°C)

V velocity (m/s)

$\dot{V}$ volume flow rate (m^3/s)

We Weber number, $\left(\frac{Q^2}{\rho_v(d_i)^3 h_{fg}^2\sigma}\right)$

Greek Symbols

ρ density (kg/m^3)

σ surface tension (N/m)

μ viscosity (Pa.s)
χ correction factor
ε effectiveness

Subscripts

a adiabatic
c condenser or cold
e evaporator
h hot
l liquid
s surface
v vapor
avg average
in input
out output
max maximum
min minimum

Reference

[1] S. Liu, J. Lia, and Q. Chen, "Visualization of flow pattern in thermosyphon by ECT," *Flow Measurement and Instrumentation*, vol.18, pp. 216–222, 2007.

[2] K.S. Ong and Md. Haider-E-Alalhi, "Experimental investigation on the hysteresis effect in vertical two-phase closed thermosyphons," *Applied Thermal Engineering*, vol. 19, pp. 399-408, 1999.

[3] T. Payakaruk, P. Terdtoon, and S. Ritthidech, "Correlations to predict heat transfer characteristics of an inclined closed two-phase thermosyphon at normal operating conditions," *Applied Thermal Engineering*, vol. 20, pp. 781-790, 2000.

[4] H. Z. Abou-Ziyan, A. Helali, M. Fatouh, and M. M. Abo El-Nasr, "Performance of stationary and vibrated thermosyphon working with water and R134a," *Applied Thermal Engineering*, vol. 21, pp. 813-830, 2001.

[5] Y. J. Park, H. K. Kang, and C. J. Kim, "Heat transfercharacteristics of a two-phase closed thermosyphon to the fill charge ratio," *International Journal of Heat and Mass Transfer*, vol. 45, pp. 4655–4661, 2002.[6] H. Farsi, J. L. Joly,

[6] M. Miscevic, V. Platel, and N. Mazet, "An experimental and theoretical investigation of the transient behavior of a two-phase closed thermosyphon," *Applied Thermal Engineering*, vol. 23, pp. 1895–1912, 2003.

[7] S. Wangnipparnto, J. Tiansuwan, T. Kiatsiriroat, and C.C. Wang, "Performance analysis of thermosyphon heat exchanger under electric field," *Energy Conversion and Management*, vol. 44, pp. 1163–1175, 2003.

[8] B. Jiao, L.M. Qiu, X.B. Zhang, and Y. Zhang, "Investigation on the effect of filling ratio on the steady-state heat transfer performance of a vertical two-phase closed thermosyphon," *Applied Thermal Engineering*, vol. 28, pp. 1417-1426, 2008.

[9] A. Alizadehdakhel, M. Rahimi, and A. A. Alsairafi, "CFD modeling of flow and heat transfer in a thermosyphon," *International Communications in Heat and Mass Transfer*, vol. 37, pp. 312-318, 2010.

[10] W. Guo and D. W. Nutter, "An experimental study of axial conduction through a thermosyphon pipe wall," *Applied Thermal Engineering*, vol. 29, pp. 3536-3541, 2009.

[11] T. Parametthanuwat, S. Rittidech, and K. Booddachan, "Thermosyphon installation for energy thrift in a smoked fish sausage oven (TISO)," *Energy*, vol. 35, pp. 2836-2842, 2010.

[12] M. Rahimi, K. Asgary, and S. Jesri, "Thermal characteristics of a resurfaced condenser and evaporator closed two-phase thermosyphon," *International Communications in Heat and Mass*

Transfer, vol. 37, pp. pp. 703-710.

[13] Z. H. Liu, Y. Y. Li, and R. Bao, "Thermal performance of inclined grooved heat pipes using nanofluids," *International Journal of Thermal Sciences*, vol. 49, pp. 1680-1687, 2010.

[14] P. Amatachaya and W. Srimuang, "Comparative heat transfer characteristics of a flat two-phase closed thermosyphon (FTPCT) and a conventional two-phase closed thermosyphon (CTPCT)," *International Communications in Heat and Mass Transfer*, vol. 37, pp. 293–298, 2010.

[15] S. Rittidech and W. Srimuang, "Correlation to predict heat-transfer characteristics of a vertical flat thermosyphon (VFT) at normal operating conditions," *International Journal of Heat and Mass Transfer*, vol. 53, pp. 5984–5987, 2010.

[16] T. Parametthanuwat, S. Rittidech, and A. Pattiya, "A correlation to predict heat-transfer rates of a two-phase closed thermosyphon (TPCT) using silver nanofluid at normal operating conditions," *International Journal of Heat and Mass Transfer*, vol. 53, pp. 4960–4965, 2010.

[17] A. R. Lukitobudi, A. Akbarzadeh, A. W. Johnson, and P. Hendy, "Design, construction and testing of a thermosyphon heat exchanger for medium temperature heat recovery in bakeries," *Heat Recovery Systems*, vol. 15 no. 5, pp. 481-491, 1995.

[18] F. Yang, X. Yuan, and G. Lin, "Waste heat recovery using heat pipe heat exchanger for heating automobile using exhaust gas," *Applied Thermal Engineering*, vol. 23, pp. 367-372, 2003.

[19] S. H. Noie and G. R. Majidian, "Waste heat recovery using heat pipe heat exchanger for surgery room in hospitals," *Applied Thermal Engineering*, vol. 20, pp. 1271-1282, 2000.

[20] S. H. Noie, "Investigated the thermal performance of an air to air thermosyphon heat exchanger," *Applied Thermal Engineering*, vol. 26, pp. 559-567, 2006.

[21] A. Y. Cengel, *Heat and mass transfer a practical approach*, 3rd ed., New York: McGraw-Hill, 2006.

[22] A. Zukauskas, "Heat transfer from tube in cross flow," *In handbook of single phase convective heat transfer*, Eds. S. Kakac, R. K. Shah, and Win Aung. New York: Wiley Interscience, 1987.

[23] R. M. Mendez, K. T. Sen, and R. M. Yang, "Effect of fin spacing on convection in a plate fin and tube heat exchanger," *International Journal Heat Mass Transfer*, vol. 43, pp. 39–51, 2000.

[24] C. C. Wang and K. Y. Chi, "Heat transfer and friction characteristics of plain fin-and-tube heat exchangers, part I: new experimental *data*," *International Journal Heat Mass Transfer*, vol. 43, pp. 2681–2691, 2000.

[25] Y. B. Tao, Y. L. He, J. Huang, Z. G. Wu, and W. Q. Tao, "Three dimensional numerical study of wavy fin-and-tube heat exchangers and field synergy principle analysis," *International Journal of Heat and Mass Transfer*, vol. 50, pp. 1163–1175, 2000.

[26] Y. B. Tao, Y. L. He, J. Huang, Z. G. Wu, and W. Q. Tao, "Numerical study of local heat transfer coefficient and fin efficiency of wavy fin-and-tube heat exchangers," *International Journal of Thermal Sciences*, vol. 46, pp. 768–778, 2007.

[27] J. Dong, J. Chen, Z. Chen, and Y. Zhou, "Air-side thermal hydraulic performance of offset strip fin aluminum heat exchangers," *Applied Thermal Engineering*, vol. 27, pp. 306-313, 2007.

[28] S. B. Riffat and G. Gan, "Determination of effectiveness of heat-pipe heat recovery for naturally-ventilated buildings," *Applied Thermal Engineering*, vol. 18, pp. 121-130, 1998.